Biogeosciences Discuss., 9, 11885–11924, 2012
www.biogeosciences-discuss.net/9/11885/2012/
doi:10.5194/bgd-9-11885-2012


Biogeosciences Discussions



# Element budgets in an Arctic mesocosm $CO_2$ perturbation study

**J. Czerny[1], K. G. Schulz[1], T. Boxhammer[1], R. G. J.Bellerby[2,4,5], J. Büdenbender[1], A. Engel[1], S. A. Krug[1], A. Ludwig[1], K. Nachtigall[1], G. Nondal[5], B. Niehoff[6], A. Siljakova[2,3], and U. Riebesell[1]**

[1]GEOMAR – Helmholtz Centre for Ocean Research, 24105 Kiel, Germany
[2]Uni Bjerknes Centre, 5007 Bergen, Norway
[3]Bjerknes Centre for Climate Research, 5007 Bergen, Norway
[4]Geophysical Institute, University of Bergen, 5007, Norway
[5]Norwegian Institute for Water Research (NIVA), 5006 Bergen, Norway
[6]Alfred Wegener Institute for Polar and Marine Research, 27515 Bremerhaven, Germany

Received: 31 July 2012 – Accepted: 2 August 2012 – Published: 31 August 2012

Correspondence to: J. Czerny (jczerny@geomar.de)

Published by Copernicus Publications on behalf of the European Geosciences Union.







## Abstract

Recent studies on the impacts of ocean acidification on pelagic communities have identified changes in carbon to nutrient dynamics with related shifts in elemental stoichiometry. In principle, mesocosm experiments provide the opportunity of determining the temporal dynamics of all relevant carbon and nutrient pools and, thus, calculating elemental budgets. In practice, attempts to budget mesocosm enclosures are often hampered by uncertainties in some of the measured pools and fluxes, in particular due to uncertainties in constraining air/sea gas exchange, particle sinking, and wall growth. In an Arctic mesocosm study on ocean acidification using KOSMOS (**K**iel **O**ff-**S**hore **M**esocosms for future **O**cean **S**imulation) all relevant element pools and fluxes of carbon, nitrogen and phosphorus were measured, using an improved experimental design intended to narrow down some of the mentioned uncertainties. Water column concentrations of particulate and dissolved organic and inorganic constituents were determined daily. New approaches for quantitative estimates of material sinking to the bottom of the mesocosms and gas exchange in 48 h temporal resolution, as well as estimates of wall growth were developed to close the gaps in element budgets. Future elevated $pCO_2$ was found to enhance net autotrophic community carbon uptake in 2 of the 3 experimental phases but did not significantly affect particle elemental composition. Enhanced carbon consumption appears to result in accumulation of dissolved organic compounds under nutrient recycling summer conditions. This carbon over-consumption effect becomes evident from budget calculations, but was too small to be resolved by direct measurements of dissolved organics. The out-competing of large diatoms by comparatively small algae in nutrient uptake caused reduced production rates under future ocean $CO_2$ conditions in the end of the experiment. This $CO_2$ induced shift away from diatoms towards smaller phytoplankton and enhanced cycling of dissolved organics was pushing the system towards a retention type food chain with overall negative effects on export potential.





BGD
9, 11885–11924, 2012



## 1 Introduction

Increasing atmospheric $CO_2$ concentration is the major man-made geochemical perturbation characterising the anthropocene (Doney, 2010; Revelle and Suess, 1957). A 40 % increase of atmospheric $CO_2$ partial pressure since the industrialisation is observed today, while rates of $CO_2$ emissions are continuing to increase beyond most modelled worst-case scenarios, e.g. SRES A1FI (Meehl et al., 2007; Friedlingstein et al., 2010). Global warming, a result of increasing $CO_2$ concentrations, is predictable and documented by current measurements as well as in the geological record (Hansen et al., 2006; Petit et al., 1999). About one third of the currently emitted $CO_2$ is dissolving in the world oceans, serving as a buffer for global climate change (Sabine et al., 2004). However, most of the absorbed $CO_2$ is accumulating in the surface ocean, separated from deep water masses by thermal stratification, that will strengthen further under global warming. In surface waters, ocean carbonation (increasing $CO_2$ concentrations) and consequential ocean acidification (decreasing pH) are affecting marine organisms thereby modulating ecosystem functioning (Riebesell et al., 2009). A predominant geochemical function of the marine planktonic ecosystem is the formation of organic matter from dissolved $CO_2$. Sinking of this organic matter, transporting carbon across barriers of physical mixing into the ocean interior is referred to as the biological carbon pump (Sarmiento and Le Quéré, 1996; Volk and Hoffert, 1985). Increasing temperatures affect the ocean as a physical $CO_2$ sink, but surface ocean warming, acidification and carbonation are also likely to impact future biological carbon sequestration (Riebesell and Tortell, 2011; Gruber, 2011).

The Arctic Ocean plays a key role in sequestration of anthropogenic carbon for several reasons. On the physical side high solubility of $CO_2$ in cold water leads to a high physical sequestration potential of anthropogenic $CO_2$ in areas of deep water formation. On the biological side high nutrient supply to the surface layer during winter deep mixing can promote pulses of high productivity with a large potential for carbon export via the biological pump (Lutz et al., 2007). Whether there is a net release or





BGD
9, 11885–11924, 2012



sequestration of atmospheric carbon depends on the carbon to nutrient ratio and sinking rate of the material exported after a mixing event. These properties are known to be highly variable, depending on the food web structure. Deep sedimentation events may occur when diatom blooms coagulate (Klaas and Archer, 2002) or pteropods and there sticky nets lead to the formation of fast sinking particles (Bathmann et al., 1991). But often efficient recycling of material by a surface layer retention food chain is keeping export at a low level (von Bodungen et al., 1995). Ocean warming and acidification are expected to impact ecosystems particularly in Arctic regions. Sea surface warming will likely result in elevated primary production due to a reduction of sea ice cover and the shoaling of mixed layer depth in the light limited Arctic. Estimates for these effects of sea surface warming are implemented in global carbon flux models (Sarmiento et al., 2004), whereas effects of changing seawater carbonate chemistry and pH on the Arctic community export production are difficult to quantify.

Ocean acidification and carbonation have the potential to directly affect ecosystem functioning in numerous ways. Of those the adverse effect of future decreasing carbonate ion concentrations on marine calcification is the most investigated mechanism (Riebesell, 2004; Fabry et al., 2008). Pteropods and foraminifera, the only calcifying organisms of significant relevance to the pelagic ecosystem examined in this study, were found to be very sensitive to ocean acidification (Comeau et al., 2009; Lombard et al., 2010; Lischka et al., 2011). Carbonation is also found to directly affect photoautotrophic carbon fixation of cultured marine phytoplankton and natural plankton assemblages (Riebesell and Tortell, 2011). In most studies, elevated $CO_2$ is reported to enhance carbon fixation but the $CO_2$ affinity of different algal taxonomic groups differs (Reinfelder, 2011). In addition to effects of ocean carbonation on primary production, bacterial enzymatic rates were found to be directly affected by decreasing seawater pH (Piontek et al., 2010). Moreover, chemical speciation of potentially limiting micronutrients seems to be pH dependent in the range of projected ocean acidification (Millero et al., 2009). Considering the various ways for ocean acidification or carbonation potentially being





BGD
9, 11885–11924, 2012



relevant for biological processes, representation of the community response in terms of carbon fluxes is difficult.

Increased inorganic carbon consumption in response to elevated $pCO_2$ was already found in incubated natural plankton communities of the North Atlantic (Hein and Sand-Jensen, 1997) and in mesocosm studies in a Norwegian Fjord compiled by Riebesell et al. (2008). $CO_2$ induced overconsumption of carbon that was presumably exuded by phytoplankton cells in form of organic matter was measured as transparent exopolymer particles (TEP). The sticky carbon-rich TEP aggregated with other particles in the water column, thereby potentially increasing carbon export (Engel, 2002; Engel et al., 2004a). Enrichment of carbon relative to nitrogen in the exported matter would cause a substantial increase in the total amount of carbon sequestered in the future ocean (Oschlies, 2009).

This study investigates the response of a natural Arctic plankton community containing all trophic levels from bacteria to millimetre-sized zooplankton, to changes in seawater $CO_2$ concentrations. Treatment levels ranged from ~ 180 µatm $CO_2$, as prevailing during the early summer situation in the beginning of the experiment, over present day and year 2100 atmospheric projections to extreme values of up to 1450 µatm $CO_2$. Using tracer gas exchange measurements and quantitative high resolution sediment sampling we are able to present daily budget calculations for carbon, nitrogen, and phosphorus in all mesocosms. Mass balance calculations, enabled us to crosscheck measured trends and to provide quantitative evaluation of biogeochemical fluxes. $CO_2$ induced changes in carbon fluxes within the water column, towards export and in exchange with the atmosphere are detected using correlation statistics. Interpretation of biogeochemistry is done in the context of the observed plankton community succession and production with special respect on carbon export fluxes at future elevated $CO_2$ concentrations.





BGD
9, 11885–11924, 2012



## 2 Material and methods

### 2.1 Experimental setup

Nine KOSMOS mesocosms were moored in the Kongsfjord, Svalbard (78°56.2′ N, 11°53.6′ E). The enclosures were cylindrical polyurethane bags two meters in diameter, 17 m long and reaching ~ 15 m deep into the water. The bags were supported by a stainless steel and glass fibre flotation frame and weighted at the bottom with steel rings closable with polycarbonate watertight shutters. The bags reaching two meters above the water surface were open to the atmosphere. A spiked roof was mounted at the top to prevent birds resting on the structures introducing nutrients into the system (Fig. 1). The fjord water, enclosed on 31 May 2010 (t-7), had a salinity of about 34 and low melt water influenced stratification. It was containing a natural plankton community whereas larger plankton and nekton were excluded using a net (3 mm mash size) covering the upper and lower opening of the mesocosms during filling. After simultaneous watertight closure of the systems on t-5, funnel type sediment traps (2 m high) covering the entire bottom surface (3.14 $m^2$) were unfolding themselves supported by a flotation ring (Fig. 1). This upper ring of the funnel had the same diameter as the bag (2 m) and was therefore touching it on all sides. The tight fit of the funnel was chosen to minimise sediment losses at the sides but resulted in ~ 4.5 $m^3$ of water below the funnel which had only limited exchange with the bulk of enclosed water above the funnel. Depending on water/bag movement water exchange between mesocosms and this "dead volume" happened on a timescale of days. Sediment lost into this dead volume was observed by divers to be very low; nonetheless changing concentrations of dissolved substances (e.g. manipulations) in the water column had to mix with this dead volume before reliable budgets could be measured. For more detail on setup see Riebesell et al. (2012) and find detailed information on abiotic conditions and standing stock succession of dissolved and particulate substances in Schulz et al. (2012).





BGD
9, 11885–11924, 2012



## 2.2 Manipulation

The water volume enclosed in the bags was determined using small additions of a calibrated NaCl solution ($\sim 1\,ml\,l^{-1} = 0.2\,g\,l^{-1}$) as a tracer. Salinity measurements allowed a calculation of the enclosed water volume with uncertainties of less than 1 % (Czerny et al., 2012a). The replicate measured volumes of all single mesocosms (t-4 and t4) could than be used to plan further manipulation steps and as a reference for budget calculations. From t-1 to t4 $CO_2$ enriched filtered seawater solution was added to achieve eight $CO_2$ treatments between 185 and 1420 µatm $CO_2$, denoting a pH gradient of 8.31 to 7.51 (measured after mixing with the dead volume on t8). The two 185 µatm $CO_2$ "control" mesocosms were undersaturated with respect to atmospheric $CO_2$ at the time the setup was deployed and were blank manipulated using 55 µm filtered fjord water. All mesocosms were enriched with $\sim 50\,nmol\,kg^{-1}$ of $N_2O$ as a deliberate gas exchange tracer on t4 when the second salt addition was performed. Early on t13, a seawater based mixed nutrient solution calculated for the volumes of the single mesocosm was added to establish equal concentrations of nitrate ($+5\,\mu mol\,kg^{-1}$), phosphate ($+0.3\,\mu mol\,kg^{-1}$) and silica ($+2.5\,\mu mol\,kg^{-1}$) in all mesocosms. All additions were performed using the "Spider" injection system (Fig. 1a). For a more detailed description of the mesocosm manipulation technique see Riebesell et al. (2012). And for description of inorganic nutrient succession see Schulz et al. (2012).

## 2.3 Sampling

Daily water sampling for dissolved and particulate parameters used for budget calculations was performed using integrating water samplers (IWS, Hydrobios, Kiel, Germany) that delivered one mixed sample representative for the upper 12 m of the water column. Immediately after water collection, gas samples for $N_2O$ and carbonate chemistry were filled directly from the sampler into gastight bottles. Samples for particulate and dissolved substances were sub-sampled in the laboratory from 20 l canisters. Canisters were transported protected from direct sunlight using black foil.





BGD
9, 11885–11924, 2012



Sediment was sampled every second day using (10 mm inner Ø) silicone tubes installed at the mesocosms reaching from the tip of the sediment funnel outside the bag to the surface (Fig. 1). Sediment suspended in water was brought up by applying a hand pumped low vacuum on a glass bottle connected to the silicone tube. Back in the laboratory particles were concentrated by settling and centrifugation in order to achieve a compact pellet that could be frozen at −80 °C.

### 2.4 Measurement procedures

Particulate matter for analyses of chlorophyll *a* (Chl *a*), particulate carbon (PC), particulate organic nitrogen (PON), biogenic silica (BSi) and phosphorus (POP) was collected by low vacuum filtration (200mbar) on glass fibre filters (Whatman GF/F 25 mm Ø pre-combusted 450 °C, 5 h) and stored frozen at −20 °C. Chl *a* was determined fluorometrically according to Welschmeyer (1994) using a Turner flourometer 10-AU (Turner BioSystems, CA, USA). Quantification of PC and PON was carried out using an elemental analyser (EuroVektor EA) according to Sharp (1974). POP and BSi was determined following the method by Hansen and Koroleff in Grasshoff et al. (1983). For POP the method was modified to the measurement of samples on glass fibre filters. Here, biomass was completely oxidised by heating the filters in 50 ml glass bottles with 40 ml of purified water and the reagent Oxisolv (Merck) in a pressure cooker. Solutions were measured colorimetrically on a Hitachi U 2000 spectrophotometer. Dissolved organic carbon (DOC), nitrogen (DON) and phosphorus (DOP) was determined from filtered (Whatman GF/F 25 mm Ø pre-combusted 450 °C, 5 h) water samples. DOC was analysed on a Shimadzu $TOC_{VCN}$ using the HTCO method. For details see Engel et al. (2012). DON and DOP were oxidised as described for POP and subsequently measured as inorganic nutrients, for nitrate ($NO_3$), nitrite ($NO_2$) and phosphate ($PO_4$) according to Hansen and Koroleff (1999) and for ammonia ($NH_4^+$) according to Holmes et al. (1999). The sum of $NO_3$, $NO_2$ and $NH_4$ is presented as dissolved inorganic nitrogen (DIN). For a more detailed description of particulate matter (POM) and dissolved organic matter (DOM) and inorganic matter (DIM) analyses see Schulz et





BGD
9, 11885–11924, 2012



al. (2012). Dissolved inorganic carbon (CT) was determined via coulorimetric titration using a SOMMA system and total alkalinity (TAlk) via potentiometric titration (Dickson, 1981). $CO_2$ concentrations, partial pressures and pH (total scale) were calculated from CT and TAlk measurements with the program CO2SYS by E. Lewis and D. Wallace (1998). For more details on carbonate chemistry see Bellerby et al. (2012).

Frozen sediment pellets were slowly (1–2 days) freeze dried and subsequently grinded in a stainless steel ball mill at low temperatures using liquid nitrogen to cool the sample before grinding. Subsamples (5–10 mg) adjusted to the analytic measurement range were weighted in on a precision scale. Analyses of particulate matter were performed as described above for PC, PON, POP and BSi on filters.

### 2.5 $CO_2$ gas exchange estimate

Daily air/sea gas exchange velocities were estimated using $N_2O$ as a deliberate tracer. Daily $CO_2$ fluxes were calculated implementing measured $CO_2$ gradients between the mesocosms and the atmosphere and correction for chemical enhancement by Hoover and Berkshire (1969). For a detailed discussion on gas exchange measurements in mesocosms see Czerny et al. (2012b).

### 2.6 Wall growth estimate

On the last days of the experiment (t30) a special brush (Fig. 1b) was used to mechanically remove and suspend biomass growing on the inner surface of the mesocosm bag as described in Riebesell et al. (2012). This biomass was than quantified by POM measurements from the water column.

### 2.7 Data presentation

Budget calculations for carbon (C), nitrogen (N) and phosphorus (P) are based on changes in pool sizes over time (Δpool) relative to a reference point in time. As the earliest reference point for C budgets we chose t8, the day at which equilibration between





BGD
9, 11885–11924, 2012



the water column above and the dead volume below the sediment traps was achieved and measured CT concentrations stabilized (after $CO_2$ manipulation). For N and P, budget calculations start on t13 after inorganic nutrients were added. As a reference value for ΔDIN and ΔDIP, from t13 onwards, concentrations measured on t12 plus the known amounts of added inorganic nutrients are used. This reference point was chosen because this way budget calculation can be started on the day of nutrient addition, e.g. before the added nutrients were fully mixed into the dead volume below the sediment traps (see Sect. 2.1). For dissolved and particulate organic C, N and P, starting values for the three phases (t8, t13, t20 for Phases I, II and III, respectively) were obtained by averaging measured concentrations of the respective days with those of the days before and after. As measurement precision for inorganic C, N and P is much higher than for particulate material, averaging over three consecutive days was not needed and the concentrations of DIM measured on the reference days were used as starting values.

Measured changes in inorganic C, N and P that can not be accounted for by the combined changes in pools of dissolved and particulate organics, cumulative gas exchange and sedimentation were assigned as "Pool X", representing a combination of measurement errors and the following pools unaccounted for in our measurements: (1) as the collecting cup of the sediment trap at 15 m water depth was 3 m below the depth range sampled by our integrating water samplers (0–12 m), sedimented particles were sampled later than their disappearances from the sampled water column. (2) A small amount of sedimented material accumulated in the space surrounding the sediment trap (dead volume) and was not sampled. (3) A biofilm growing on the mesocosm walls became visible towards the end of the experiment. The size of this pool was estimated from water column measurements taken immediately before and after brushing the mesocosm walls. (4) Fast swimming zooplankton such as copepods were not quantitatively sampled with the depth integrating sampler and are therefore not adequately represented in PC/PON / POP measurements. Biomass of zooplankton larger than 55 µm was estimated by weekly Apstein net hauls. (5) Dissolved organic C and





BGD
9, 11885–11924, 2012



N measurements as well as particulate organic P were excluded from mass balance calculation because measurement uncertainties of these parameters were larger than the size of Pool X (see Fig. 3b) and would therefore compromise mass balance calculations. Corrections for evaporation on dissolved and particulate matter concentrations as well as corrections for sampling-derived volume decrease on the normalisation of fluxes on seawater volume were not included to keep calculations traceable. With a range of ∼0.2 % and ∼1 % respectively over the whole experiment corrections are below the detection limit of most of the applied methods.

Pool X for C, N and P ($\Delta X_{C/N/P}$) were calculated using the following equations:

$$\Delta X_C = \Delta CT + \Delta GX + \Delta PC + \Delta Sed_C$$

$$\Delta X_N = \Delta DIN + \Delta PON + \Delta Sed_N$$

$$\Delta X_P = \Delta DIP + \Delta DOP + \Delta Sed_P$$

ΔCT = Change in total dissolved inorganic carbon, ΔDIP = Change in dissolved inorganic phosphorus concentrations in the water column, ΔDIN = Change in dissolved inorganic nitrogen concentrations in the water column, ΔGX = Cumulative exchange of carbon with the atmosphere (flux in = negative/out = positive), ΔPC = Change in total particulate carbon concentrations in the water column, ΔPON = Change in particulate organic nitrogen concentrations in the water column, ΔDOP = Change in dissolved organic phosphorus concentrations in the water column, ΔSed = Cumulative amounts of the respective element found in the sediment trap.

As sediment traps were sampled every second day, obtained values were linearly interpolated for days without measurements. Also missing data points of other parameters were linearly interpolated between preceding and subsequent measurements. This applies for DON and DOP of all mesocosms on t16 and t19 and 8 single data points of DOC.





BGD
9, 11885–11924, 2012



### 2.8 Statistics

The setup with eight different $CO_2$ treatment levels and no replication of treated mesocosms was designed for regression analyses. Delta values of all tested phases are calculated using the first day of the respective phase as a reference point. Means of changes in measurement parameters (Δvalues) of single mesocosms during the three phases of the experiment were plotted against mean $pCO_2$ in the mesocosms during that specific phase. The null hypothesis that the overall slope is zero and that there is no linear relationship between treatment $pCO_2$ and mean Δvalues was statistically tested with an F-test. Data satisfied assumptions for normal distribution, as confirmed by a Shapiro-Wilk-Test. Analyses were performed using the program Statistica 6.0 (StatSoft Inc., Tulsa, USA).

## 3 Results

### 3.1 Chlorophyll *a* and the analysed phases of the experiment

The experiment can be divided into three phases of autotrophic bloom development. An increase in Chl *a* (Fig. 2) started in all mesocosms already during $CO_2$ manipulation and peaked on t7. This first bloom was mainly supported by residual concentrations of inorganic phosphorus and ammonium as well as dissolved organic nitrogen (DON), see Schulz et al. (2012). A $CO_2$ effect on Chl *a* concentrations during Phase I was not observed. After nutrient addition (t13), there was a lag phase of 2 to 3 days until Chl *a* started to increase. Phase I carbon budget calculation starts on t8, just after the Phase I peak, and is thus describing processes during the bloom decay until t15. During Phase II, from t13 onwards, large parts of the added inorganic nutrients were consumed and budgets for C, N and P were calculated for build-up and decay of the second bloom peak until t20. Here, the peak Chl *a* of the high $CO_2$ treatments was higher than that at intermediate and low $CO_2$ levels. During Phase III, starting on t20, Chl *a* at low and





BGD
9, 11885–11924, 2012



intermediate $CO_2$ started to increase exponentially, reaching maximum concentrations on t27 and declining thereafter. In contrast, in high $pCO_2$ treatments Chl *a* increased more slowly, not reaching peak values until the end of the experiment.

Maximal Chl *a* concentrations of $\sim 3\,\mu g\,l^{-1}$ during the course of the experiment are rather low in consideration of $5\,\mu mol\,kg^{-1}$ nitrate and $0.32\,\mu mol\,kg^{-1}$ phosphate added. Chl *a* concentrations were transformed into estimates of organic carbon for the autotrophic community using Chl *a*/carbon ratios by (Li et al., 2010), with 0.02 gChl *a* $gC^{-1}$ for the first peak owing to a low contribution of diatoms and a ratio of 0.036 gChl *a* $gC^{-1}$ for the Phase III peak, when diatoms were abundant. Transformation reveals that the contribution of the photoautotrophic biomass (2 to $8\,\mu mol\,kg^{-1}$ C) to the standing stock of particulate carbon (PC) (up to $40\,\mu mol\,kg^{-1}$) was rather small.

### 3.2 Carbon budget of the replicated control treatment

In Fig. 3 carbon pools of the untreated control mesocosms are plotted over the entire period of the experiment. The bloom development as displayed in Chl *a* (Fig. 2) is mirrored by build-up of ΔPC and cumulative sedimentation of this biomass (Fig. 3a). Until t8, autotrophic uptake of inorganic carbon resulted in a simultaneous decrease of ΔCT which was partly compensated by in-gassing of $CO_2$ from the atmosphere. Hereafter biomass decreased and PC was partly respired back into the CT pool, sedimenting out or being released as DOC. Three days after the addition of inorganic nutrients (t16) up until t19 ΔPC build up combined with sedimentation was not leading to changes in ΔCT but was compensated by $CO_2$ entering the mesocosm from the atmosphere. During these 19 days the sum of particulate carbon produced in the control mesocosms roughly equals the sum of inorganic carbon consumed, indicated by Pool X being close to zero for this period. Measured DOC values are included to this calculation in Fig. 3b. Apparently, day-to-day variability in this data set is much larger than the amount of carbon potentially available for the formation of DOC. This is evident from the sum of other measured carbon species shown as Pool X in Fig. 3a. Similar, unexplained variability as in DOC measurements was also found for DON and POP, so that changes in





BGD
9, 11885–11924, 2012



these pools are estimated from Pool X calculated from those parameters which were measured at reasonable precision.

As shown in Fig. 3c, the temporal development of the missing carbon fraction Pool X in the two control treatments was very similar. Variability of Pool X during most of the experimental time was relatively small (Pool X is on average $-0.43 \pm 2.7$ µmol kg$^{-1}$ for the two controls until t19). From t19 to t27, a bloom took place in the mesocosms, extensively consuming inorganic carbon. Increasing ΔPC values and cumulative sedimentation do not balance the sum of 44 µmol kg$^{-1}$ inorganic carbon taken up from the dissolved pool plus the $CO_2$ entered from the atmosphere. A Pool X value of 19 µmol kg$^{-1}$ is, therefore, required to close the carbon budget at t27. Within this period biomass growing attached to the walls became visible and was estimated to account for 7.3 µmol kg$^{-1}$ of Pool X on t30 averaged over all mesocosms. Visual inspections by divers indicated that large parts of the visible wall growth was removed by the brushing, but measurements most likely underestimate the actual wall growth.

### 3.3 $CO_2$ effects on carbon budgets

Changes in inorganic carbon concentrations between t8 and t27 (Fig. 4a) are correlated to $CO_2$ levels with the highest $CO_2$ treatment showing the strongest decrease in CT. At high $pCO_2$ the decrease was rather linear over time whereas there was only a minor change in CT concentrations in the low $CO_2$ treatments during the first 12 days of this period. Most of these $CO_2$ related differences were caused by gas exchange with the atmosphere. One third (24 µmol kg$^{-1}$) of the CT decrease at the highest $CO_2$ can be attributed to outgassing, whereas about 10 µmol kg$^{-1}$ atmospheric carbon entered the lowest $CO_2$ treatments (Fig. 4b). The gas exchange corrected variation of ΔCT (Fig. 4c), $\Delta CT_{GX}$, is an approximation for net organic carbon fixation as calcification was negligible during the experiment (Silyakova et al., 2012). Approximately equal amounts of inorganic carbon were consumed biologically in all treatments, between t8 and t27. However, the dynamic of carbon uptake over time strongly differed among $CO_2$





BGD
9, 11885–11924, 2012



treatments. CT was taken up immediately and rather continuously at high $CO_2$. At low $CO_2$ there was a considerable lag phase until t20 but than net uptake rates exceeded rates at high $CO_2$, so that all treatments ended up with similar overall uptake at the end of Phase III. Overall ΔPC build-up calculated from t8, with maximal 10 µmol $kg^{-1}$ (Fig. 4d), was rather small compared to net carbon uptake $\Delta CT_{GX}$ of ~40 µmol $kg^{-1}$. Cumulative sedimentation can only account for half as much as ΔPC build-up (up to 5 µmol $kg^{-1}$, Fig. 4e). As the build-up of both measured particulate carbon species cannot explain the measured drawdown in $\Delta CT_{GX}$, the loss fraction Pool X is accumulating over time (Fig. 4f).

### 3.4 Phase I

By separating the budget into the 3 phases of the experiment, uptake and production in the 9 mesocosms can be directly compared using regression analyses. As inorganic nutrients were low at the beginning of Phase I, there was no uptake and inorganic nutrient budgets were not calculated. However, $\Delta CT_{GX}$ (Fig. 5a) shows a relatively strong decrease of inorganic carbon at high $CO_2$ compared to net heterotrophic production at low $CO_2$. This highly significant $CO_2$ effect on carbon uptake is not reflected in particulate carbon accumulation (Fig. 5b, Table 1). ΔPC was decreasing from the t8 bloom peak, while sedimentation was equally low in all treatments. This translates into a significant positive correlation of ΔPool X to $CO_2$ in Phase I (Table 1), causing an offset at high $CO_2$ that persisted over most of the experimental time (Fig. 4f).

### 3.5 Phase II

During Phase II, dissolved inorganic matter (DIM), comprising inorganic carbon concentrations (Fig. 5d) together with inorganic nutrients, decreased significantly stronger at high $CO_2$ (Table 1). Although statistical tests could not detect a significant $CO_2$ related increase in all pools of dissolved and particulate organic matter, significant positive trends in Chl *a* (Fig. 2), ΔPON, ΔDOP, and ΔDOC (as Pool X; Fig. 5h, Table 1)





BGD
9, 11885–11924, 2012



suggest a general positive growth effect of $CO_2$ during Phase II. Budgets indicate that the surplus carbon, taken up at high $CO_2$, accumulated in the dissolved organic pool, while nitrogen remained mainly in the particulate fraction and phosphorus was almost equally partitioned between both the particulate and dissolved organic fraction (Table 1 and Supplement). The small sedimentation event peaking on t16 can be mainly allocated to cirripedia larvae migrating into the sediment trap (Figs. 6a, 5g). The settling of these meroplanktonic larvae decreased meta zooplankton biomass by 40–60 % (from overall average $5.0 \pm 1.8$ to $3.1 \pm 1.1$ µmol $kg^{-1}$) over the course of the experiment, thereby contributing ~ 60 % of the export flux during Phases I and II (see also Niehoff et al. (2012). However, a sedimentation event caused by pteropods introduced into the mesocosm during Phase I was not detected. The animal density of ~ 4 pteropods $m^{-3}$ (Riebesell et al., 2012) was very low compared to abundances of more than 13 000 $m^{-3}$ observed to cause sedimentation events in the Arctic (Bathmann et al., 1991). The fairly large dead individuals were excluded from the sediment samples.

### 3.6 Phase III

In Phase III the $CO_2$-related trends in DIM uptake rates of Phase II were reversed. Significantly more inorganic carbon was consumed at low $CO_2$ (Fig. 5i), resulting in significantly stronger build-up of PC (Fig. 5j) and export of this material (Fig. 5k). Pool X (Fig. 5l) was steadily increasing until day 27 in all $CO_2$ treatments. Major parts of the nutrients added on t13 accumulated in Pool X until the end of the experiment on t30 (averaged ~ 55 % for N and 74 % for P). On average 16 % of added N and 32 % of added P was measured in the form of wall growth on t30. A $CO_2$ effect on wall growth seems possible but is not indicated by direct measurements on t30 or by Pool X. Trends in inorganic carbon uptake during Phase III are parallel to trends in uptake of inorganic nutrients (Table 1). As inorganic N and P were supplied in the beginning of Phase II in equal concentrations (5 µmol $kg^{-1}$ N, 0.32 µmol $kg^{-1}$ P), stronger uptake at high $CO_2$ during Phase II resulted in lowered concentrations of the limiting nutrient during Phase III when N and P became exhausted in all mesocosms. Uptake rates were considerably





BGD
9, 11885–11924, 2012



faster in the still relatively nutrient replete low $CO_2$ treatments. On the last day of the experiment net autotrophic growth rates at low $CO_2$ exceeded all rates observed before during this experiment. $CO_2$ related trends in ΔPC, ΔPON and especially in export of C, N and P could be clearly detected. Changes in nearly all of the particulate pools showed highly significant negative correlations to treatment $pCO_2$ (Table 1).

### 3.7 Stoichiometry of biomass

Elemental ratios of the suspended particulate organic material (averaged over all mesocosms) were always close to Redfield ratios (Fig. 7). $CO_2$ or nutrient manipulation did not cause strong changes in elemental composition of biomass. C / N and N / P ratios of material sampled from the sediment traps were generally similar to ratios obtained for suspended organic matter, with mean N / P ratios of sedimented matter slightly higher than comparative values from the water column. During the last days (t27–t30) of the experiment, C / N ratios of suspended material increased in all mesocosms (Fig. 7a). This increase was significantly stronger for the low $CO_2$ treatments. The same general increase was observed in the sediment material but here C / N started to rise already on t24, reaching higher maximum values than in the water column (Fig. 7b). Diatom aggregates contributed the largest fraction of the sedimented material during the last week of the experiment as documented by a strong increase in biogenic silica fluxes (Fig. 6b), an elevated Si / C ratio (Fig. 6c) and microscopic inspection.

## 4 Discussion

### 4.1 Phase I

In the control treatments, dynamics in dissolved inorganic carbon and gas exchange over the first 19 days of the experiment are well represented by measured production, export and respiration of particulate organic matter (Fig. 3). Systematic errors such as





BGD
9, 11885–11924, 2012



over- or underestimation of sedimentation or gas exchange seem to be small as those would have caused Pool X to gradually increase instead of fluctuating closely around zero. This implies that the carbon budged was closed for this period and that there was no significant accumulation of dissolved organic matter at low $CO_2$. At high $CO_2$, however, there was significantly higher carbon consumption during Phase I (Figs. 4c, 5a). As this extra carbon ($\sim 13\ \mu mol\ kg^{-1}$) consumed at high $CO_2$ did not show up in any of the particulate carbon pools (Fig. 5b, c), it has to be allocated to the dissolved carbon fraction (here Pool $X_C$; Figs. 4f, 5d). DOC measurements in the mesocosms were not able to quantitatively resolve this trend due to a high day-to-day variability, probably caused by contaminations of the samples (Fig. 3b). Nevertheless, statistical analyses of DOC measurements as well as $^{14}C$ DOC primary production measurements by Engel et al. (2012) support our interpretation of increased DOC production in the phase before nutrient addition. Increasing DOC was probably a result of viral lyses and grazing causing the decline of the Phase I bloom (Brussaard, 2012a). Despite a net decrease of ΔPC in all treatments, growth rates of the dominant phytoplankton were found to be high by $^{13}C$ and $^{14}C$ incorporation techniques (de Kluijver et al., 2012; Engel et al., 2012). This primary production, causing the net uptake of inorganic carbon documented by a decrease $\Delta CT_{GX}$ at high $CO_2$ (Fig. 5a), was exceeded by heterotrophy at low $CO_2$. The rapid cycling of carbon at high $CO_2$ during Phase I obviously resulted in the accumulation of dissolved organic compounds that were not consumed immediately by the bacterial community and persisted at least during Phase II, where net production of DOC was much lower (Fig. 4f). A semi-labile nature of the produced dissolved organic matter in this experiment becomes also evident from apparent substrate limitation of heterotrophic bacteria during the entire experiment, detected by Piontek et al. (2012).

The phenomenon of inorganic carbon drawdown with low net consumption of N or P, as evident at high $CO_2$ between t8 and t15, is called carbon over-consumption (Toggweiler, 1993). An enhancement of carbon consumption was already found in incubations of natural Atlantic plankton communities under high $CO_2$ (Schulz et al.,2008;





BGD
9, 11885–11924, 2012



Bellerby et al., 2008; Riebesell et al., 2007; Delille et al., 2005; Engel et al., 2004a; Egge et al., 2009; Hein and Sand-Jensen, 1997) and is also indicated by increased cumulative $^{14}C$ primary production observed during this experiment by Engel et al. (2012). The product of this enhanced photosynthetic activity was often not directly measured, but was hypothesised to be released as DOC, indicated by the occurrence of transparent exopolymer particles (TEP) (Engel et al., 2004a). Enhanced DOC relative to PC production in response to high $pCO_2$ was lately found to be further accelerated with climate warming (Kim et al., 2011). Exudation of carbon compounds by cultured microalgae as well as by natural plankton assemblages is known to vary with environmental factors such as temperature, light, nutrient availability and $CO_2$. (Marañón et al., 2004; Zlotnik and Dubinsky, 1989; Engel, 2002). Sedimentation of aggregated DOC in the form of TEP was hypothesized to be the cause for increased carbon loss under high $CO_2$ in the PEECE III study (Schulz et al., 2008) and previous experiments (Engel et al., 2004b). In the present experiment elevated TEP concentrations were measured at high $CO_2$ in the end of Phase II (Engel, 2012). This would suggest a loss of DOC, into the PC pool, but neither increased sedimentation nor increased carbon contents of sediments or of suspended PC under high $CO_2$ were measured. Thus, there is no evidence for TEP as an important aggregation factor in this study. Sugars serving as precursors for TEP were possibly produced at concentrations too low to form relevant amounts of aggregates or were consumed by the bacterial community (Piontek et al., 2010). DOC was therefore remaining in the water column, where it might have supported the development of a large microbial community competing with primary producers for inorganic nutrients and promoting enhanced shallow remineralisation of produced biomass (Thingstad et al., 2008).

### 4.2 Phase II

During Phase II trends in uptake of inorganic C, N and P after nutrient addition are consistent with trends in Chl *a*. Elevated $CO_2$ concentrations seemed to have a stimulating effect on growth of the dominating picoeukaryotic primary producers (Brussaard,





BGD
9, 11885–11924, 2012



2012b; Schulz et al., 2012), leading to increased uptake of inorganic C, N and P (Table 1, Fig. 5e) as well as increased cell numbers and Chl *a*. However, increasing biomass production as a result of enhanced nutrient uptake at high $CO_2$ during the bloom of picoeukaryotes in Phase II was hardly detectable as organic matter build up and did not cause a measurable sedimentation event (Fig. 5f, g). The peak in carbon export caused by cirripedia larvae shows that the settling of meroplankton can seasonally make up a large share of vertical fluxes in coastal ecosystems (Fig. 6a). Autotrophic biomass in the water column, estimated from Chl *a* as well as bio-volume estimates of picoeukaryotes (Brussaard, 2012b) can only account for the amount of C, N and P consumed during the first days of Phase II. Thereafter, phytoplankton standing stocks were diminished and kept at a relatively low level by grazing and viral lyses (Brussaard, 2012b) while nutrient uptake continued (Schulz et al., 2012). No significant $CO_2$ correlated differences in ΔPC as well as ΔPOP (also as Pool $X_P$) could be detected during entire Phase II (Table 1). The fact that the dissolved organic pools are indeed showing $CO_2$ related differences in DOC as Pool $X_C$ (Fig. 5h) and in ΔDOP support the hypotheses that enhanced autotrophy at high $CO_2$ was top-down controlled. In contrast to P and C enhanced uptake of inorganic nitrogen at high $CO_2$ was reflected in higher ΔPON and only minor amounts of N in Pool $X_N$ remain to be allocated to DON. Nitrogen was obviously incorporated into the heterotrophic community (Table 1).

### 4.3 Phase III

A relatively diverse phytoplankton community comprised of picoeukariotes co-dominated by diatoms and dinoflagellates established during Phase III (Schulz et al., 2012; Brussaard, 2012b). This bloom showed higher C, N and P uptake rates at low $CO_2$, whereas under high $CO_2$ uptake was already slowing down due to nutrient depletion after the Phase II peak (Fig. 5i). Reduced growth at high $CO_2$ in Phase III was reflected by significantly lower ΔPC, ΔPON, ΔPOP (Table 1). Biomass build-up resulting from fast carbon and nutrient drawdown does not seem to be limited by strong loss processes as observed in the previous two phases. Diatoms, contributing relatively low





BGD
9, 11885–11924, 2012



biomass to the water column community (Schulz et al., 2012), increasingly dominated the sedimented material from the beginning of Phase III in all treatments. This is illustrated also by BSi : C ratios, which increased from t20 onwards (Fig. 6c). Overall higher biomass build-up seemed to be causing a sedimentation event of diatoms, forming aggregates with other particles, transporting them into the sediment trap. The retention food web, quickly recycling freshly produced biomass, seems to be shifted towards an export community in Phase III (Wassmann, 1997). In this system nutrients diminished by picoeukariots at high $CO_2$ during Phase II limited biomass production that could be exported. The total amount of export production can not be calculated for this period as measurements ended before peak sedimentation rates were reached (Fig. 6a). In addition to that, wall-grown biomass, not being exported, was exponentially increasing (Fig. 3c). However, significantly less carbon uptake, PC and PON accumulation in the water column and less export of C, N and P under high $CO_2$ during Phase III was evident until nutrient depletion. As inorganic N and P were depleted by t28, a comparable export flux at high $CO_2$, occurring after the end of our measurements (t30), seems unlikely.

### 4.4 Soichiometry of exported biomass

Temporal trends in elemental composition of the sedimented material was very similar to that of the suspended matter during most of the experiment (Fig. 7). The relatively fresh material sampled in the bottom of the shallow mesocosms seemed to be an even intersection of suspended particles. However, sinking detritus and digested material of the large heterotrophic community is probably responsible for the general offset in composition of sedimenting material towards higher C / N and N / P ratios throughout the experiment. The observed increase of C / N ratios in the sedimented compared to the suspended matter during Phase III coincide with a larger fraction of freshly produced phytoplankton biomass in the settling material. Increasing sediment C / N ratios correlate with the increasing Si / C ratios (Fig. 6c), indicating that a diatom ballast or aggregation effect caused the overrepresentation of carbon rich particles in the sediments.





BGD
9, 11885–11924, 2012



The same C / N increase occurred later and less pronounced in the water column; here diatoms and fresh material, observed to be dominating the sediment samples during Phase III, are measured against a much larger background of other suspended matter diluting the signal.

There were no $CO_2$ related differences in biomass composition until nutrients were depleted on t28. On t30 higher C / N ratios at low $CO_2$ appeared in the suspended matter. This signal, albeit strongly amplified, was also apparent in the sedimented matter. Mesocosms showing stronger elevated C / N ratios on the last day yielded also higher sediment quantities of C, N, P and Si (Table 1). As the inorganic carbon dataset ends on t27, carbon uptake beyond the day of nutrient depletion was not measured, but already until t27 there seems to be higher carbon consumption at low $CO_2$ during the combined post nutrient phase (II + III) (Figs. 4c, 5e, i). Elevated C or reduced N content of the phytoplankton community might have been amplified due to growth limitation by dissolved inorganic nitrogen with concentrations below 1 µmol $kg^{-1}$ already since t24 in all treatments (Klausmeier et al., 2004).

While changes in biomass composition in response to future $CO_2$, reported from laboratory experiments on phytoplankton (Burkhardt et al., 1999; Burkhardt and Riebesell, 1997), vary between species in strength and direction, differences in organic C / N / P ratios of primary producers growing under inorganic nutrient limitation and repletion are a common phenomenon (Klausmeier et al., 2004). The fact that we did not observe strong changes during this experiment is most likely a result of the diverse composition of POM with phytoplankton comprising only a relatively small fraction during large parts of the experiment. Therefore elemental composition of POM is largely dominated by the composition of heterotrophs and detritus and even the stoichiometry of phytoplankton might have been controlled by consumer driven nutrient recycling (Elser and Urabe, 1999). Fast recycling of readily available N and P compounds ($NH_4$ / ATP) were certainly comprising a large part of the fluxes even during nutrient replete phases of the experiment. The sudden increase in biomass carbon contents accompanied by significantly elevated export rates at low $CO_2$ happened in the last days of observation





BGD
9, 11885–11924, 2012



when a switch from a strongly top-down controlled retention type to a export system occurred.

### 4.5 Synthesis

Future $CO_2$ concentrations were found to stimulate autotrophic production two times during the course of this experiment. First during Phase I when increased inorganic carbon uptake by nanoplankton at high $CO_2$ was directly channelled into dissolved organics. Secondly during Phase II when enhanced growth of picoeukaryots diminished inorganic nutrient concentrations at high $CO_2$, resulting in less organic matter being exported in Phase III. During this experiment, both positive effects on primary production had negative influence on carbon export.

It becomes clear that $CO_2$ affected ecosystem productivity and biogenic carbon fluxes are a product of complex interactions controlled by $CO_2$ or pH dependent mechanisms. However, when the dominating producers or consumers in a mesocosm have responded to the manipulation in the beginning of the experiment, any effects following up are multi-causal. Growth enhancement of nanoplankton and picoeukariots during Phase I and II was presumably causing most of the characteristic effect of $CO_2$ on bloom dynamics (Brussaard, 2012b). Therefore, e.g. direct physiological $CO_2$ effects on the community dominating within Phase III would be a matter of speculation due to the different nutrient situation already in the beginning of Phase III. Ecological data are of substantial importance in making biogeochemical response patterns comparable between experiments. Apparently, responses found for the retention type community which was present at the start of this experiment, are not directly comparable to earlier findings for export systems such as the cocolithophore blooms in Norwegian coastal waters compiled by Riebesell et al. (2008). Therefore, results and findings of these experiments have to be interpreted with caution. Community experiments always have to be seen as case studys with results primarily valid for the specific community composition enclosed at the start of the experiment. Further experiments will show whether





BGD
9, 11885–11924, 2012



$CO_2$-enhanced DOC production and growth of smaller phytoplankton can be consistently found at similar community composition.

There is first evidence that climate warming might have synergistic effects with ocean carbonation. Trends towards increased DOM production and a shift towards smaller phytoplankton found as a result of increased $pCO_2$ in this study were also shown before as a result of warming. Higher turnover of organic matter due to increased DOC production and acceleration of heterotrophic activity in response to future elevated temperatures (Wohlers et al., 2009; Engel et al., 2010) was found in mesocosms investigating Baltic plankton communities. A gradual shift towards a more diverse plankton community comprised of smaller organisms in the North Atlantic was already observed during the last decades and was attributed to shoaling of the mixed surface layer due to increasing sea surface temperatures (Beaugrand et al., 2010). First combined mesocosm experiments on climate warming and ocean acidification/carbonation showed responses by lower trophic plankton levels to add up or potentiate (Kim et al., 2011). Experiments on the combined effect of different aspects of global change on multitrophic communities have to be elaborated in the future.

Laboratory studies performed on single species are highly sensitive in detecting physiological $CO_2$ effects, whereas the importance of these effects within a natural ecosystem is always hard to estimate (Riebesell and Tortell, 2011). In this study we showed ocean acidification/carbonation to affect small phytoplankton that significantly influenced principle ecosystem functioning. Whereas the growth effect on picoeucariotes itself had no effect on carbon export fluxes and could not even be clearly detected in POM, follow up effects were indeed of biogeochemical relevance. Identifying species that have the potential to change biogeochemical fluxes by influencing community succession is an important task for future mesocosm experiments. Research on the physiology of such key ecosystem components in ocean acidification could than be intensified. Focussing down from the community to the species level instead of extrapolating from the laboratory to the filed could accelerate the progress of finding general biogeochemical response patterns.





BGD
9, 11885–11924, 2012



**Supplementary material related to this article is available online at: http://www.biogeosciences-discuss.net/9/11885/2012/ bgd-9-11885-2012-supplement.pdf.**

*Acknowledgements.* This work is a contribution to the "European Project on Ocean Acidification" (EPOCA) which received funding from the European Community's Seventh Framework Programme (FP7/2007–2013) under grant agreement no. 211384. Financial support was provided through Transnational Access funds by the European Union Seventh Framework Program (FP7/2007–2013) under grant agreement no. 22822 MESOAQUA and by Federal Ministry of Education and Research (BMBF, FKZ 03F0608) through the BIOACID (Biological Impacts of Ocean ACIDification) project. We gratefully acknowledge the logistical support of Greenpeace International for its assistance with the transport of the mesocosm facility from Kiel to Ny-Ålesund and back to Kiel. We also thank the captains and crews of M/V *ESPERANZA* of Greenpeace and R/V *Viking Explorer* of the University Centre in Svalbard (UNIS) for assistance during mesocosm transport and during deployment and recovery in Kongsfjorden. We thank the staff of the French-German Arctic Research Base at Ny-Ålesund, in particular Marcus Schumacher, for on-site logistical support.

The service charges for this open access publication have been covered by a Research Centre of the Helmholtz Association.

## References

Bathmann, U. V., Noji, T. T., and von Bodungen, B.: Sedimentation of pteropods in the Norwegian Sea in autumn, Deep Sea Res., 38, 1341–1360, 1991.

Beaugrand, G., Edwards, M., and Legendre, L.: Marine biodiversity, ecosystem functioning, and carbon cycles, P. Natl. Acad. Sci., 107, 10120–10124, doi:10.1073/pnas.0913855107, 2010.

Bellerby, R. G. J., Schulz, K. G., Riebesell, U., Neill, C., Nondal, G., Heegaard, E., Johannessen, T., and Brown, K. R.: Marine ecosystem community carbon and nutrient uptake





BGD

9, 11885–11924, 2012



stoichiometry under varying ocean acidification during the PeECE III experiment, Biogeosciences, 5, 1517–1527, doi:10.5194/bg-5-1517-2008, 2008.
Bellerby, R. G., Silyakova, A., Nondal, G., Slagstad, D., Czerny, J., De Lange, T., and Ludwig, A.: Marine carbonate system evolution during the EPOCA Arctic pelagic ecosystem experiment in the context of simulated future Arctic ocean acidification, Biogeosciences. Discuss., in preparation, 2012.
Brussaard, C.: OA effects on virolysis and grazing of bacteria, Biogeosciences. Discuss., in preparation, 2012a.
Brussaard, C.: OA impact on Arctic microbial dynamics Biogeosciences. Discuss., in preparation, 2012b.
Burkhardt, S. and Riebesell, U.: $CO_2$ availability affects elemental composition (C:N:P) of the marine diatom *Skeletonema costatum*, Mar. Ecol. Prog. Ser., 155, 67–76, doi:10.3354/meps155067, 1997.
Burkhardt, S., Zondervan, I., and Riebesell, U.: Effect of $CO_2$ concentration on the C:N:P ratio in marine phytoplankton: A species comparison., Limnol. Oceanogr., 44, 683–690, 1999.
Comeau, S., Gorsky, G., Jeffree, R., Teyssié, J.-L., and Gattuso, J.-P.: Impact of ocean acidification on a key Arctic pelagic mollusc (*Limacina helicina*), Biogeosciences, 6, 1877–1882, doi:10.5194/bg-6-1877-2009, 2009.
Czerny, J., Schulz, K. G., Krug, S. A., Ludwig, A., and Riebesell, U.: Technical note on the determination of enclosed water volume in the pelagic mesocosms "KOSMOS", Biogeosciences. Discuss, submitted, 2012a.
Czerny, J., Schulz, K. G., and Riebesell, U.: A simple method for gas exchange measurements in mesocosms and its application in mesocosm carbon budget calculations, Biogeosciences. Discuss., accepted, 2012b.
de Kluijver, A., Soetaert, K., Czerny, J., Schulz, K. G., Boxhammer, T., Riebesell, U., and Middelburg, J. J.: A 13C labelling study on carbon fluxes in Arctic plankton communities under elevated $CO_2$ levels, Biogeosciences Discuss., 9, 8571–8610, doi:10.5194/bgd-9-8571-2012, 2012.
Delille, B., Harlay, J., Zondervan, I., Jacquet, S., Chou, L., Wollast, R., Bellerby, R. G. J., Frankignoulle, M., Borges, A. V., Riebesell, U., and Gattuso, J.-P.: Response of primary production and calcification to changes of $pCO_2$ during experimental blooms of the coccolithophorid Emiliania huxleyi, Global Biogeochem. Cy., 19, GB2023, doi:10.1029/2004gb002318, 2005.





BGD
9, 11885–11924, 2012



Doney, S. C.: The Growing Human Footprint on Coastal and Open-Ocean Biogeochemistry, Science, 328, 1512–1516, doi:10.1126/science.1185198, 2010.
Egge, J. K., Thingstad, T. F., Larsen, A., Engel, A., Wohlers, J., Bellerby, R. G. J., and Riebesell, U.: Primary production during nutrient-induced blooms at elevated CO2 concentrations, Biogeosciences, 6, 877–885, doi:10.5194/bg-6-877-2009, 2009.
Elser, J. J. and Urabe, J.: The stoichiometry of consumer-driven nutrient recycling: Theory, observations, and consequences, Ecology, 80, 735–751, 1999.
Engel, A.: Direct relationship between $CO_2$ uptake and transparent exopolymer particles production in natural phytoplankton, J. Plankton Res., 24, 49–53, 2002.
Engel, A.: OA effects on carbohydrates, amino acids and gel particles Biogeosciences. Discuss., in preparation, 2012.
Engel, A., Delille, B., Jacquet, S., Riebesell, U., Rochelle-Newall, E., Terbrüggen, A., and Zondervan, I.: Transparent exopolymer particles and dissolved organic carbon production by Emiliania huxleyi exposed to different $CO_2$ concentrations: a mesocosm experiment, Limnol. Oceanogr, 50, 493–507, 2004a.
Engel, A., Thoms, S., Riebesell, U., Rochelle-Newall, E., and Zondervan, I.: Polysaccharide aggregation as a potential sink of marine dissolved organic carbon, Nature, 428, 929–932, 2004b.
Engel, A., Händel, N., Wohlers, J., Lunau, M., Grossart, H.-P., Sommer, U., and Riebesell, U.: Effects of sea surface warming on the production and composition of dissolved organic matter during phytoplankton blooms: results from a mesocosm study, J. Plankton Res., 33, 357–372, doi:10.1093/plankt/fbq122, 2010.
Engel, A., Borchard, C., Piontek, J., Schulz, K., Riebesell, U., and Bellerby, R.: $CO_2$ increases $^{14}C$-primary production in an Arctic plankton community, Biogeosciences Discuss., 9, 10285–10330, doi:10.5194/bgd-9-10285-2012, 2012.
Fabry, V. J., Seibel, B. A., Feely, R. A., and Orr, J. C.: Impacts of ocean acidification on marine fauna and ecosystem processes, ICES Journal of Marine Science, 65, 414–432, doi:10.1093/icesjms/fsn048, 2008.
Friedlingstein, P., Houghton, R. A., Marland, G., Hackler, J., Boden, T. A., Conway, T. J., Canadell, J. G., Raupach, M. R., Ciais, P., and Le Quéré, C.: Update on $CO_2$ emissions, Nat. Geosci, 3, 811–812, 2010.
Grasshoff, K., Ehrhardt, M., and Kremling., K.: Methods of Seawater Analysis., 2 ed., Verlag Chemie, Weinheim, Germany, 1983.





BGD
9, 11885–11924, 2012



Gruber, N.: Warming up, turning sour, losing breath: ocean biogeochemistry under global change, Philosophical Transactions of the Royal Society A: Mathematical, Phys. Eng. Sci., 369, 1980–1996, doi:10.1098/rsta.2011.0003, 2011.
Hansen, H. and Koroleff, R.: Methods of Seawater Analysis, edited by: Grasshoff, K., Kremmling, K., and Ehrhardt, M., Wiley, Weinheim, Germany, 159–228, 1999.
Hansen, J., Sato, M., Ruedy, R., Lo, K., Lea, D. W., and Medina-Elizade, M.: Global temperature change, P. Natl. Acad. Sci., 103, 14288–14293, doi:10.1073/pnas.0606291103, 2006.
Hein, M. and Sand-Jensen, K.: $CO_2$ increases oceanic primary production, Nature, 388, 526–527, 1997.
Holmes, R. M., Aminot, A., Kerouel, R., Hooker, B. A., and Peterson, B. J.: A simple and precise method for measuring ammonium in marine and freshwater ecosystems, Can. J. Fish Aquat. Sci., 56, 1801–1808, doi:10.1139/f99-128, 1999.
Hoover, T. E. and Berkshire, D. C.: Effects of Hydration on Carbon Dioxide Exchange across an Air-Water Interface, J. Geophys. Res., 74, 456–464, doi:10.1029/JB074i002p00456, 1969.
Kim, J.-M., Lee, K., Shin, K., Yang, E. J., Engel, A., Karl, D. M., and Kim, H.-C.: Shifts in biogenic carbon flow from particulate to dissolved forms under high carbon dioxide and warm ocean conditions, Geophys. Res. Lett., 38, L08612, doi:10.1029/2011GL047346, 2011.
Klaas, C. and Archer, D. E.: Association of sinking organic matter with various types of mineral ballast in the deep sea: Implications for the rain ratio, Global Biogeochem. Cy., 16, 1116, doi:10.1029/2001gb001765, 2002.
Klausmeier, C., Litchman, E., and Levin, S.: Phytoplankton growth and stoichiometry under multiple nutrient limitation, Limnol. Oceanogr., 49, 1463–1470, 2004.
Lewis, E. and Wallace, D. W. R.: Program developed for CO2 system calculations. ORNL/CDIAC-105, Carbon Dioxide Information Center, Oak Ridge National Laboratory, US Department of Energy, Oak Ridge, Tennessee, 1998.
Li, Q. P., Franks, P. J. S., Landry, M. R., Goericke, R., and Taylor, A. G.: Modeling phytoplankton growth rates and chlorophyll to carbon ratios in California coastal and pelagic ecosystems, J. Geophys. Res., 115, G04003, doi:10.1029/2009jg001111, 2010.
Lischka, S., Büdenbender, J., Boxhammer, T., and Riebesell, U.: Impact of ocean acidification and elevated temperatures on early juveniles of the polar shelled pteropod Limacina helicina: mortality, shell degradation, and shell growth, Biogeosciences, 8, 919–932, doi:10.5194/bg-8-919-2011, 2011.





BGD
9, 11885–11924, 2012



Lombard, F., da Rocha, R. E., Bijma, J., and Gattuso, J.-P.: Effect of carbonate ion concentration and irradiance on calcification in planktonic foraminifera, Biogeosciences, 7, 247–255, doi:10.5194/bg-7-247-2010, 2010.

Lutz, M. J., Caldeira, K., Dunbar, R. B., and Behrenfeld, M. J.: Seasonal rhythms of net primary production and particulate organic carbon flux to depth describe the efficiency of biological pump in the global ocean, J. Geophys. Res., 112, C10011, doi:10.1029/2006jc003706, 2007.

Marañón, E., Cermeño, P., Emilio, F., Rodríguez, J., and Zabala, L.: Significance and mechanisms of photosynthetic production of dissolved organic carbon in a coastal eutrophic ecosystem, Limnol. Oceanogr., 49, 1652–1666, 2004.

Meehl, G. A. S., T. F., Collins, W. D., Friedlingstein, A. T., Gaye, A. T., Gregory, J. M., Kitoh, A., Knutti, R., Murphy, J. M., Noda, A., Raper, S. C. B., Watterson, I. G., Weaver, A. J., and Zhao, Z.: Global climate projections, in: Climate Change 2007, The physical science basis, edited by: Solomon, S., Qin, D., and Manning, M., Technical support unit, IPCC working group 1, Cambridge University Press, 748–845, 2007.

Millero, F. J., Woosley, R., DiTrolio, B., and Waters, J.: Effect of Ocean Acidification on the Speciation of Metals in Seawater, Oceanography, 22, 72–85, 2009.

Niehoff, B., Knüppel, N., Daase, M., Czerny, J., and Boxhammer, T.: Mesozooplankton community development at elevated $CO_2$ concentrations: Results from a mesocosm experiment in a high Arctic fjord, Biogeoscience Discuss., in press, 2012.

Oschlies, A.: Impact of atmospheric and terrestrial $CO_2$ feedbacks on fertilization-induced marine carbon uptake, Biogeosciences, 6, 1603–1613, doi:10.5194/bg-6-1603-2009, 2009.

Petit, J. R., Jouzel, J., Raynaud, D., Barkov, N. I., Barnola, J.-M., Basile, I., Bender, M., Chappellaz, J., Davis, M., Delaygue, G., Delmotte, M., Kotlyakov, V. M., Legrand, M., Lipenkov, V. Y., Lorius, C., P.Épin, L., Ritz, C., Saltzman, E., and Stievenard., M.: Climate and atmospheric history of the past 420,000 years from the Vostok ice core, Antarctica, Nature, 399, 429–436, 1999.

Piontek, J., Lunau, M., Händel, N., Borchard, C., Wurst, M., and Engel, A.: Acidification increases microbial polysaccharide degradation in the ocean, Biogeosciences, 7, 1615–1624, doi:10.5194/bg-7-1615-2010, 2010.

Piontek, J., Borchard, C., Sperling, M., Schulz, K. G., Riebesell, U., and Engel, A.: Response of bacterioplankton activity in an Arctic fjord system to elevated $pCO_2$: results from a mesocosm





BGD
9, 11885–11924, 2012



perturbation study, Biogeosciences Discuss., 9, 10467–10511, doi:10.5194/bgd-9-10467-2012, 2012.
Reinfelder, J. R.: Carbon Concentrating Mechanisms in Eukaryotic Marine Phytoplankton, Ann. Rev. Mar. Sci., 3, 291–315, doi:10.1146/annurev-marine-120709-142720, 2011.
Revelle, R. and Suess, H. E.: Carbon Dioxide Exchange Between Atmosphere and Ocean and the Question of an Increase of Atmospheric $CO_2$ during the Past Decades, Tellus, 9, 18–27, doi:10.1111/j.2153-3490.1957.tb01849.x, 1957.
Riebesell, U.: Effects of $CO_2$ Enrichment on Marine Phytoplankton, J. Oceanogr., 60, 719–729, 2004.
Riebesell, U., Schulz, K. G., Bellerby, R. G., Botros, M., Fritsche, P., Meyerhöfer, M., Neill, C., Nondal, G., Oschlies, A., Wohlers, J., and Zöllner, E.: Enhanced biological carbon consumption in a high $CO_2$ ocean., Nature, 450, 545–548, 2007.
Riebesell, U., Bellerby, R. G. J., Grossart, H.-P., and Thingstad, F.: Mesocosm $CO_2$ perturbation studies: from organism to community level, Biogeosciences, 5, 1157–1164, doi:10.5194/bg-5-1157-2008, 2008.
Riebesell, U., Körtzinger, A., and Oschlies, A.: Sensitivities of marine carbon fluxes to ocean change, P. Natl. Acad. Sci., 106, 20602–20609, doi:10.1073/pnas.0813291106, 2009.
Riebesell, U. and Tortell, P. D.: Effects of ocean acidification on pelagic organisms and ecosystems, in: Ocean Acidification, edited by: Gattuso, J. P. and Hanson, L., Oxford University Press, Oxford, 99–121, 2011.
Riebesell, U., Czerny, J., von Bröckel, K., Boxhammer, T., Büdenbender, J., Deckelnick, M., Fischer, M., Hoffmann, C., Krug, S. A., Lenz, U., Ludwig, A., Muche, R., and Schulz, K. G.: A mobile sea-going mesocosm system: new opportunities for ocean change research, Biogeosciences. Discuss., in preparation, 2012.
Sabine, C. L., Feely, R. A., Gruber, N., Key, R. M., Lee, K., Bullister, J. L., Wanninkhof, R., Wong, C. S., Wallace, D. W. R., Tilbrook, B., Millero, F. J., Peng, T.-H., Kozyr, A., Ono, T., and Rios, A. F.: The Oceanic Sink for Anthropogenic $CO_2$, Science, 305, 367–371, doi:10.1126/science.1097403, 2004.
Sarmiento, J. L. and Le Quéré, C.: Oceanic Carbon Dioxide Uptake in a Model of Century-Scale Global Warming, Science, 274, 1346–1350, doi:10.1126/science.274.5291.1346, 1996.
Sarmiento, J. L., Slater, R., Barber, R., Bopp, L., Doney, S. C., Hirst, A. C., Kleypas, J., Matear, R., Mikolajewicz, U., Monfray, P., Soldatov, V., Spall, S. A., and Stouffer, R.: Re-





BGD
9, 11885–11924, 2012



sponse of ocean ecosystems to climate warming, Global Biogeochemical Cy., 18, GB3003, doi:10.1029/2003GB002134, 2004.
Schulz, K. G., Riebesell, U., Bellerby, R. G. J., Biswas, H., Meyerhöfer, M., Müller, M. N., Egge, J. K., Nejstgaard, J. C., Neill, C., Wohlers, J., and Zöllner, E.: Build-up and decline of organic matter during PeECE III, Biogeosciences, 5, 707–718, doi:10.5194/bg-5-707-2008, 2008.
Schulz, K. G., Bellerby, R. G. J., Brussaard, C., Büdenbender, J., Czerny, J., Fischer, M., Koch-Klavsen, S., Krug, S. A., Lischka, S., Ludwig, A., Meyerhöfer, M., Nondal, G., Silyakova, A., Stuhr, A., and Riebesell, U.: Temporal biomass dynamics of an Arctic plankton bloom in response to increasing levels of atmospheric carbon dioxide, Biogeosciences. Discuss., in preparation, 2012.
Sharp, J. H.: Improved analysis for "particulate" organic carbon and nitrogen from seawater, Limnol. Oceanogr., 19, 984–989, 1974.
Silyakova, A., Bellerby, R. G. J., Czerny, J., Schulz, K. G., Nondal, G., Tanaka, T., Engel, A., De Lange, T., and Riebesell, U.: Net community production and stoichiometry of nutrient consumption in a pelagic ecosystem of a northern high latitude fjord: mesocosm $CO_2$ perturbation study, Biogeosciences Discuss., 9, 11705–11737, doi:10.5194/bgd-9-11705-2012, 2012.
Thingstad, T. F., Bellerby, R. G. J., Bratbak, G., Borsheim, K. Y., Egge, J. K., Heldal, M., Larsen, A., Neill, C., Nejstgaard, J., Norland, S., Sandaa, R. A., Skjoldal, E. F., Tanaka, T., Thyrhaug, R., and Topper, B.: Counterintuitive carbon-to-nutrient coupling in an Arctic pelagic ecosystem, Nature, 455, 387–390, 2008.
Toggweiler, J. R.: Carbon overconsumption, Nature, 363, 210–211, 1993.
Volk, T. and Hoffert, M. I.: Ocean carbon pumps – Analyses of reactive strengths and efficiencies in ocean-driven atmospheric $CO_2$ changes, in: The Carbon Cycle and Atmospheric $CO_2$: Natural Variations, Archean to Present, edited by: Sundquist, E. and Broecker, W., AGU Geophysical Monograph, Washington DC, 99–110, 1985.
von Bodungen, B., Antia, A., Bauerfeind, E., Haupt, O., Koeve, W., Machado, E., Peeken, I., Peinert, R., Reitmeier, S., Thomsen, C., Voss, M., Wunsch, M., Zeller, U., and Zeitzschel, B.: Pelagic processes and vertical flux of particles: an overview of a long-term comparative study in the Norwegian Sea and Greenland Sea, Geol. Rundsch., 84, 11–27, doi:10.1007/bf00192239, 1995.
Wassmann, P.: Retention versus export food chains: processes controlling sinking loss from marine pelagic systems, Hydrobiologia, 363, 29–57, doi:10.1023/a:1003113403096, 1997.





BGD
9, 11885–11924, 2012



Welschmeyer, N. A.: Fluorometric analysis of chlorophyll a in the presence of chlorophyll b and pheopigments, Limnol. Oceanogr., 29, 1985–1992, 1994.
Wohlers, J., Engel, A., Zöllner, E., Breithaupt, P., Jürgens, K., Hoppe, H.-G., Sommer, U., and Riebesell, U.: Changes in biogenic carbon flow in response to sea surface warming, Proc. Natl. Acad. Sci., 106, 7067–7072, doi:10.1073/pnas.0812743106, 2009.
Zlotnik, I. and Dubinsky, Z.: The effect of light and temperature on DOC excretion by phytoplankton, Limnol. Oceanogr., 34, 831–839, 1989.





BGD
9, 11885–11924, 2012



**Table 1.** Results of F-test (regression analyses) testing for $CO_2$ dependent changes in pool sizes of C, N and P during the three phases of the experiment. Analysed delta values for each phase are calculated using the first day of the respective phase as a reference point. Mean delta concentrations of the elements in particulate organic (POM), dissolved inorganic (DIM) and dissolved organic matter (DOM) as well as cumulative sediments (Sed.) and the missing fraction (Pool X) were plotted against mean $CO_2$ concentrations during the phase. Significant trends ($p<0.05$) are marked in bold. Direction (Dir) of trends are given for correlations $p<0.1$. N stands for negative correlation to $pCO_2$ and would for example mark a significantly stronger decrease in DIM with increasing $pCO_2$ wile P stands for positive correlation to $pCO_2$ and could therefore mark significantly increasing concentrations, for example, POM with increasing $pCO_2$.

| Testet period | | ΔPOM | | | ΔDIM | | | ΔDOM | | | Sed. | | | ΔPool X | | |
|---|---|---|---|---|---|---|---|---|---|---|---|---|---|---|---|---|
| | | $r^2$ | $p$ | Dir | $r^2$ | $p$ | Dir | $r^2$ | $p$ | Dir | $r^2$ | $p$ | Dir | $r^2$ | $p$ | Dir |
| Phase 1 | Carbon | | | | | | | | | | | | | | | |
| | T8–T15 | 0.01 | 0.78 | – | **0.98** | **<0.00** | **N** | 0.42 | 0.06 | P | 0.02 | 0.75 | – | **0.96** | **<0.00** | **P** |
| Phase 2 | Carbon | | | | | | | | | | | | | | | |
| | T14–T21 | 0.27 | 0.15 | – | **0.92** | **<0.00** | **N** | 0.01 | 0.77 | – | 0.00 | 0.92 | – | **0.66** | **0.01** | **P** |
| | Nitrogen | | | | | | | | | | | | | | | |
| | T14–T21 | **0.52** | **0.03** | **P** | **0.87** | **<0.00** | **N** | 0.25 | 0.17 | – | 0.02 | 0.69 | – | 0.07 | 0.50 | – |
| | Phosphorous | | | | | | | | | | | | | | | |
| | T14–T21 | 0.35 | 0.10 | – | **0.93** | **<0.00** | **N** | **0.54** | **0.02** | **P** | 0.02 | 0.71 | – | 0.13 | 0.34 | – |
| Phase 3 | Carbon | | | | | | | | | | | | | | | |
| | T21–T27 | **0.86** | **<0.00** | **N** | **0.85** | **<0.00** | **P** | 0.07 | 0.49 | – | **0.65** | **0.01** | **N** | 0.35 | 0.09 | N |
| | Nitrogen | | | | | | | | | | | | | | | |
| | T21–T30 | **0.83** | **<0.00** | **N** | **0.89** | **<0.00** | **P** | 0.13 | 0.35 | – | **0.63** | **0.01** | **N** | 0.25 | 0.17 | – |
| | Phosphorous | | | | | | | | | | | | | | | |
| | T21–T30 | 0.31 | 0.12 | – | **0.94** | **<0.00** | **P** | 0.15 | 0.31 | – | **0.64** | **0.01** | **N** | **0.47** | **0.04** | N |





BGD
9, 11885–11924, 2012



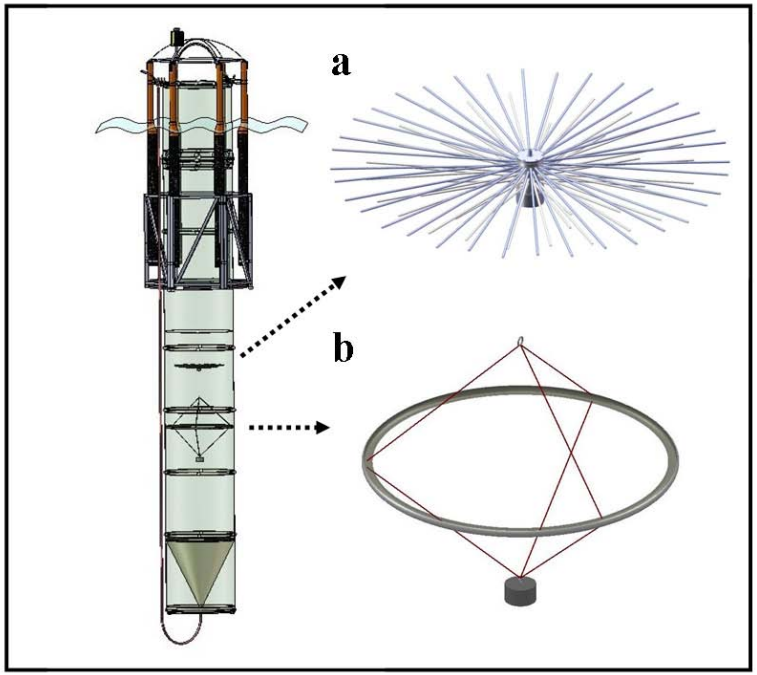


**Fig. 1.** Sketch of one of the nine experimental units. Total view of the mesocosm with **(a)** manipulation device "Spider" and **(b)** wall brush.





BGD
9, 11885–11924, 2012



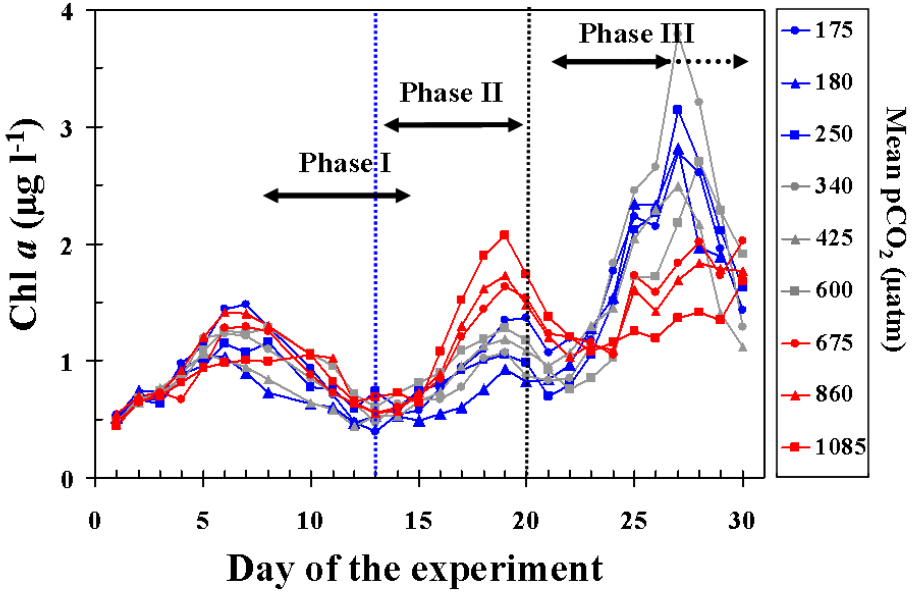


**Fig. 2.** Development of chlorophyll *a* concentrations during the course of the experiment. High $pCO_2$ are denoted in red, intermediate in grey and low levels in blue. Within these categories circles symbolise the lowest, triangles intermediate and squares the highest treatment level. The blue dashed line marks the nutrient addition (t13) at the end of Phase I. The black dashed line denotes the end of Phase II comprising the second bloom peak, Phase III corresponds to the third bloom until the end of measurements. Arrows depict time periods used for statistical analyses.





BGD
9, 11885–11924, 2012



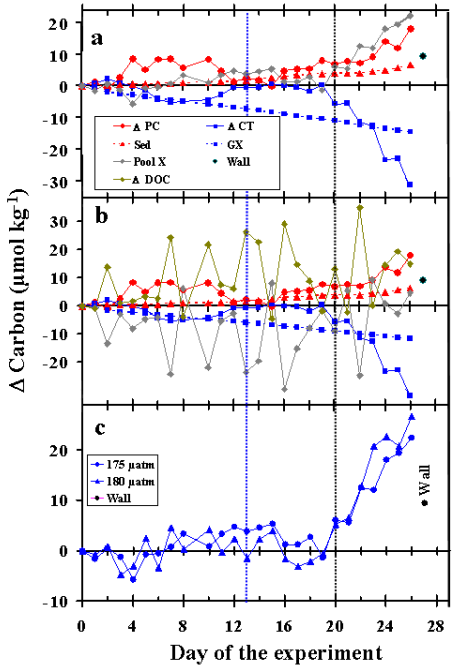


**Fig. 3.** Temporal development of carbon pools in the control treatments. Panel **(a)** shows daily measured differences in particulate carbon (ΔPC), dissolved inorganic carbon (ΔCT), cumulative sedimented carbon (Sed) and $CO_2$ gas exchange (GX) relative to day zero for the lowest $CO_2$ treatment (175 µatm). Pool X is the fraction that can not be accounted for by changes in the above mentioned pools. In panel **(b)** measured changes in dissolved organic carbon (ΔDOC) are included. Panel **(c)** compares Pool X of the 175µatm treatment with Pool X of the 180 µatm parallel treatment. Black dots plotted after the data series represent the mean amount of wall growth among all treatments measured at the end of the experiment (t30). The black dashed line denotes the end of Phase II comprising the second bloom peak; Phase III corresponds to the third bloom until the end of measurements.





BGD
9, 11885–11924, 2012



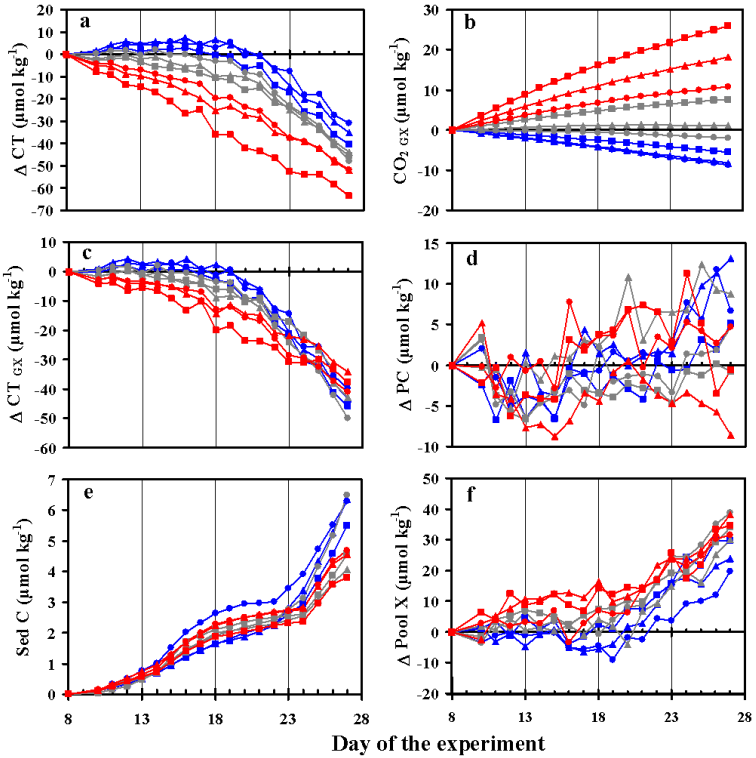


**Fig. 4.** Temporal development of carbon pools in all treatments relative to day 8. Sedimentation (Sed) **(e)** is shown cumulative. Changes in particulate carbon (ΔPC) **(d)** are measured differences to day 8 values while biologically mediated changes in inorganic carbon concentrations ($\Delta CT_{GX}$) shown in **(c)** are (ΔCT) **(a)** corrected for gas exchange $CO_{2\ GX}$ **(b)**. Pool X is the sum of ($\Delta CT_{GX}$), (ΔPOC) and (Sed) and accounts for the carbon allocated to (DOC) and undetermined pools (see Sect. 2.7).





BGD
9, 11885–11924, 2012



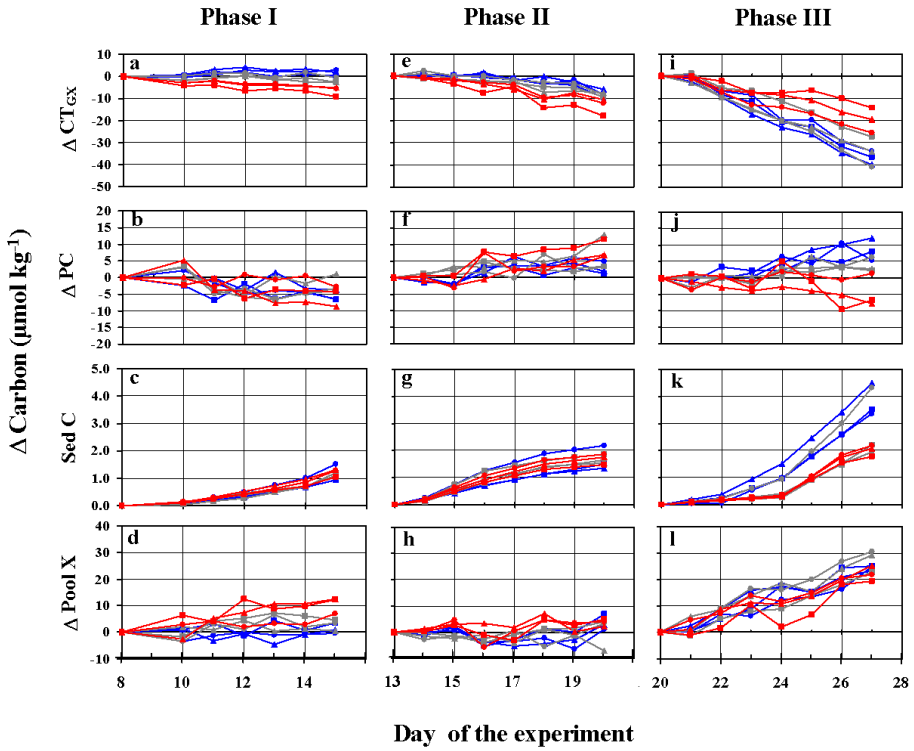


**Fig. 5.** Temporal development of carbon pools in all treatments for the three phases of the experiment. Sedimentation (Sed) is shown cumulative. Changes in particulate carbon (ΔPC) are measured differences to start values while biologically mediated changes in inorganic carbon concentrations ($\Delta CT_{GX}$) correspond to (ΔCT) corrected for gas exchange. Pool X is the sum of ($\Delta CT_{GX}$), (ΔPOC) and (Sed) and accounts for the carbon allocated to (DOC) and undetermined pools (see Sect. 2.7).





BGD
9, 11885–11924, 2012



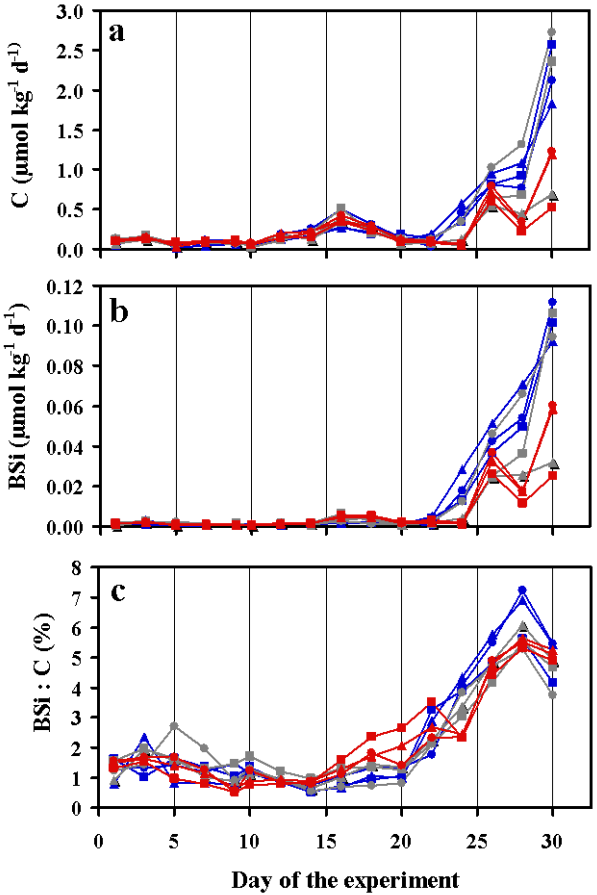


**Fig. 6.** Vertical fluxes for carbon **(a)** and biogenic silica **(b)** normalised to kg seawater and day. Biogenic silica to carbon ratios in the sedimented material are shown in panel **(c)**.





BGD
9, 11885–11924, 2012



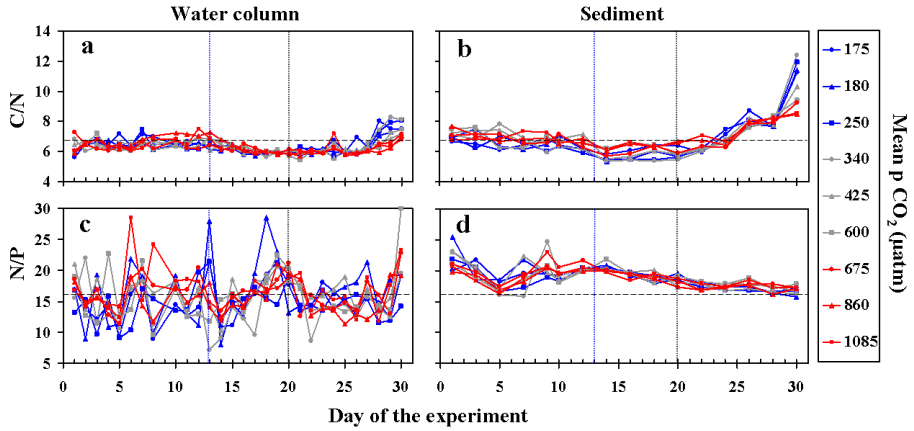


**Fig. 7.** Temporal development of carbon to nitrogen (C / N) and nitrogen to phosphorus (N / P) ratios of particles suspended in the water column (left) and particles sampled in the sediment traps (right). Dashed horizontal line marks Redfield ratios. $CO_2$ partial pressures given in the figure legend are mean values for the experiment (day 8–26). Vertical dashed lines are coded as described for Fig. 2.





BGD
9, 11885–11924, 2012